Key Points:
- The ^{233}U/^{236}U ratio and the ^{236}U composition unravel Pacific and Atlantic waters in Polar Surface Waters of the western Arctic Ocean
- The Atlantic Layer exhibit distinct ^{233}U and ^{236}U signals from Polar Surface Waters
- Deep and Bottom Waters show extremely low ^{233}U and ^{236}U concentrations with isotopic ratios distinct from known anthropogenic U sources

Correspondence to:
E. Chamizo and M. Christl,
echamizo@us.es;
mchristl@phys.ethz.ch

The Potential of ^{233}U/^{236}U as a Water Mass Tracer in the Arctic Ocean

E. Chamizo[1] , **M. Christl[2]** , **M. López-Lora[1,3]** , **N. Casacuberta[2,4]** , **A.-M. Wefing[2,4]** , and **T. C. Kenna[5]**

[1]Centro Nacional de Aceleradores (CNA), Universidad de Sevilla, Junta de Andalucía, Consejo Superior de Investigaciones Científicas, Sevilla, Spain, [2]Laboratory of Ion Beam Physics, Institute for Particle Physics and Astrophysics, ETH Zürich, Zürich, Switzerland, [3]Department of Health, Medicine and Caring Sciences (HMV), Linköping University, Linköping, Sweden, [4]Environmental Physics, Institute of Biogeochemistry and Pollutant Dynamics, ETH Zürich, Zurich, Switzerland, [5]Lamont-Doherty Earth Observatory, Columbia University, Palisades, NY, USA

Abstract This study explores for the first time the possibilities that the ^{233}U/^{236}U atom ratio offers to distinguish waters of Atlantic or Pacific origin in the Arctic Ocean. Atlantic waters entering the Arctic Ocean often carry an isotopic signature dominantly originating from European reprocessing facilities with some smaller contribution from global fallout nuclides, whereas northern Pacific waters are labeled with nuclides released during the atmospheric nuclear testing period only. In the Arctic Ocean, ^{233}U originates from global fallout while ^{236}U carries both, a global fallout and a prominent nuclear reprocessing signal. Thus, the ^{233}U/^{236}U ratio provides a tool to identify water masses with distinct U sources. In this work, ^{233}U and ^{236}U were analyzed in samples from the GN01 GEOTRACES expedition to the western Arctic Ocean in 2015. The study of depth profiles and surface seawater samples shows that: (a) Pacific and Atlantic waters show enhanced signals of both radionuclides, which can be unraveled based on their ^{233}U/^{236}U signature; and (b) Deep and Bottom Waters show extremely low ^{233}U and ^{236}U concentrations close to or below analytical detection limits with isotopic ratios distinct from known anthropogenic U sources. The comparably high ^{233}U/^{236}U ratios are interpreted as a relative increase of naturally occurring ^{233}U and ^{236}U and thus for gradually reaching natural ^{233}U/^{236}U levels in the deep Arctic Ocean. Our results set the basis for future studies using the ^{233}U/^{236}U ratio to distinguish anthropogenic and pre-anthropogenic U in the Arctic Ocean and beyond.

Plain Language Summary We study the presence of ^{233}U and ^{236}U in seawater samples taken in the Arctic Ocean from the GN01 GEOTRACES expedition in 2015. Both long-lived manmade U isotopes were introduced worldwide during the open-air testing of nuclear weapons (mainly in the 1960s). ^{236}U is also linked to the civil uses of nuclear energy, particularly to the liquid effluents from Sellafield (United Kingdom) and La Hague (France) reprocessing plants (starting in the 1950s). Atlantic Waters flowing into the Arctic Ocean carry both the bomb-tests and the reprocessing plants signals. Pacific Waters entering the Arctic Ocean carry the bomb-tests signal only. Thus, they show different ^{233}U and ^{236}U compositions. We demonstrate that the ^{233}U/^{236}U ratio and the ^{236}U composition can be used to identify water masses of Pacific and Atlantic origin in the upper waters of the western Arctic Ocean. Deep and Bottom Waters, where an anthropogenic influence is not expected, exhibit extremely low ^{233}U and ^{236}U concentrations but ^{233}U/^{236}U ratios above the ones observed in the upper Arctic Ocean. These features can be explained by the presence of naturally produced uranium isotopes of lithogenic origin. This study demonstrates the potential of the ^{233}U/^{236}U ratio to distinguish anthropogenic and natural U in the Arctic Ocean and beyond.

1. Introduction

Since the 1980s, a variety of chemical tracers have shed light on the circulation patterns and mixing processes of Pacific Waters (PW) and Atlantic Waters (AW) in the Arctic Ocean (AO). Natural tracers such as nitrate and phosphate concentrations (E. Peter Jones et al., 1998), and new tracers like Ga (Whitmore et al., 2020), are used to distinguish the interface between PW and AW in the upper water column of the AO. Artificial tracers such as chlorofluorocarbons (CFCs) and ^{3}H (T$_{1/2}$ = 12.33 years) have been used to understand the lateral transport of AW in the AO. CFCs have been introduced into the surface ocean via gas exchange since the 1950s with mostly increasing input functions (Bullister, 2014; Tanhua et al., 2009), while a ^{3}H pulse originating from atmospheric nuclear bomb testing (i.e., from 1945 to 1980, peaking in the 1960s) has rained down on the ocean's surface

Funding acquisition: T. C. Kenna
Investigation: E. Chamizo, M. Christl, M. López-Lora
Project Administration: N. Casacuberta
Resources: E. Chamizo, M. Christl, N. Casacuberta, T. C. Kenna
Supervision: M. Christl, N. Casacuberta
Validation: E. Chamizo, M. López-Lora
Visualization: M. López-Lora
Writing – original draft: E. Chamizo
Writing – review & editing: M. Christl, M. López-Lora, N. Casacuberta, A.-M. Wefing

(Dorsey & Peterson, 1976; Weiss & Roether, 1980). Both above tracers have been applied in the North Atlantic to estimate ventilation rates of deep waters (Doney et al., 1997). In addition to the global release of radionuclides during the atmospheric bomb tests (global fallout, GF), the nuclear reprocessing plants (RPs) of Sellafield and La Hague have fingerprinted AW and added artificial radionuclides to the AO. For example, the fission by-products ^{137}Cs ($T_{1/2} = 30.07$ years) and ^{129}I ($T_{1/2} = 15.7$ My) have been used to get insights into circulation patterns and transit times of AW in the AO (Smith et al., 2011; Tanhua et al., 2009). Today, the AO is experiencing critical changes that are rapidly affecting its unique properties such as ice-cover and density structure of the water column. PW and hence freshwater export from the AO is subject to temporal variations and plays an important role for deep-water formation in the subpolar North Atlantic (Holliday et al., 2020; Rahmstorf et al., 2015). Conventional tracers used to study PW in the AO are subject to ongoing discussion, since the resulting PW fractions show a large variation (Alkire et al., 2015, 2019). Exploring new tracers that provide novel or complementary information on PW fractions and the general role of PW and AW in influencing or even driving changes in the AO water column is a key aspect for understanding and predicting the role of the AO in global climate change (Årthun et al., 2019; Woodgate et al., 2010).

^{236}U ($T_{1/2} = 23.4$ My) has been used in the last few years to track pathways and timescales of AW within the AO. As a chemical tracer, ^{236}U has three key properties: it can be assumed to be conservative in seawater as the naturally occurring isotope ^{238}U (Aya Sakaguchi et al., 2012; Dunk et al., 2002); its radioactive decay is negligible in the time frame of the oceanic processes of interest in the AO; and its main source terms to the AO are traceable and time-dependent, which can be used to estimate pathways and circulation timescales. ^{236}U is produced by the interaction of ^{235}U (^{238}U) with thermal (fast) neutrons (Sakaguchi et al., 2009). Thus, it is present globally as a consequence of the GF, and regionally in the North Atlantic Ocean and AO mostly due to the liquid releases from Sellafield and La Hague RPs (Casacuberta et al., 2016, 2018). It has been estimated that RPs have released about 250 kg of ^{236}U to the Irish and North Seas since the 1950s (Castrillejo et al., 2020). The worldwide budget of GF ^{236}U is roughly 1,000 kg (Sakaguchi et al., 2009; Winkler et al., 2012). Yet, only small fractions of those budgets have entered the AO. About 8 kg of GF ^{236}U (assuming an average atmospheric deposition of 1.13×10^{12} at/m^2 for the 70–90° latitude range (Hardy et al., 1973; Sakaguchi et al., 2009)) was directly deposited on the surface of the AO during the nuclear testing period. That budget has been significantly increased since then due to the inflow of AW and PW (i.e., waters from mid latitudes that have seen a much higher direct atmospheric deposition of bomb-tests nuclides), continental runoff and precipitation. ^{236}U has been widely redistributed in the AO through the complex water masses currents system. Therefore, studying ^{236}U concentrations alone does not provide clear information on its sources. To overcome this problem, in the last few years, ^{236}U has been used in combination with ^{129}I in a dual tracer approach (Wefing et al., 2021).

Recently, the study of another minor U isotope, ^{233}U ($T_{1/2} = 0.159$ My), in Greenland Sea surface waters, has set the basis to the use of ^{233}U/^{236}U as a tool to disentangle anthropogenic U sources and thus trace water masses in the AO (Qiao, Hain, & Steier, 2020). Unlike ^{236}U, ^{233}U ($T_{1/2} = 0.159$ My) is not produced in significant amounts in conventional nuclear reactors running on uranium fuel and providing a thermal neutron spectrum (Ho et al., 2019). Theoretical estimations point to ^{233}U/^{236}U atom ratios at the level of 10^{-6} in burned nuclear fuel (Naegeli, 2004), and values ranging from about 6×10^{-8} to 5×10^{-7} have been documented for La Hague RP releases ("HELCOM MORS Discharge database," n.d.). This implies that releases from Sellafield and La Hague RPs would account for a total of less than 0.5 g of anthropogenic ^{233}U. On the other hand, significant amounts of ^{233}U were released worldwide during the atmospheric nuclear testing period due to a series of weapons with specific designs (i.e., by those either using ^{233}U as the fissile material or by those thermonuclear devices containing a tamper of ^{235}U in which ^{233}U is produced in ^{235}U(n, 3n) reactions with fast neutrons (Hain et al., 2020)). To date, the most accurate estimation of the GF ^{233}U/^{236}U atom ratio based on a peatbog core from Germany is $(1.40 \pm 0.15) \times 10^{-2}$ (Hain et al., 2020). Assuming this ratio can be extrapolated to other latitudes, about 14 kg of ^{233}U would have been globally dispersed during the atmospheric testing of nuclear weapons. A minor fraction of this GF ^{233}U would be present today in the AO, mostly due to its transport away from the Arctic and by dilution with inflowing AW and PW. Former Soviet Union thermonuclear tests at Novaya Zemlya, among them the largest one ever conducted, of 50 Mt in 1961 (UNSCEAR., 2000), could have also contributed to the regional ^{233}U budget in the AO. Although most of that signal would have already left the AO with outflowing waters (Wefing et al., 2021), a part of it might still be present in ice sheets or in the AO river catchments, thus potentially influencing the current ^{233}U (and ^{236}U) budget in the AO. Due to a lack of information on the ^{233}U content of the above
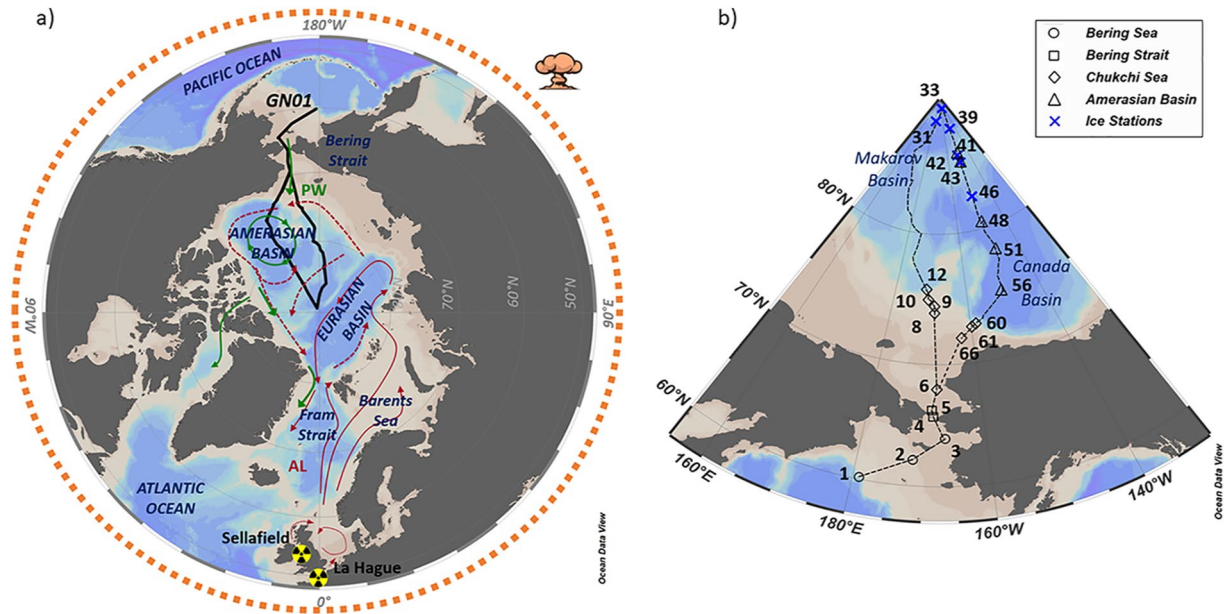
Figure 1. (a) Situation of the GEOTRACES GN01 transect with the main pathways of Pacific Waters (PW, in green) and Atlantic Waters (AW, in red) currents circulating at surface in the Arctic Ocean, and (b) sampling stations grouped by geographical areas.

sources we considered them included in the GF source term. Thus, the ^{233}U/^{236}U ratio, involving two radionuclides with distinct sources, could be used to get more insights into the presence of anthropogenic U in the AO.

With respect to the use of this ratio as a water mass tracer, a further advantage is represented by the fact that two isotopes of the same element behave geochemically identical (and conservatively in the U case) in seawater. Therefore, ^{233}U/^{236}U has the potential to become a robust water mass tracer that is less sensitive to many mixing processes with tracer-free waters. A direct application would be the study of the mixing between PW and AW: while nuclear testing period ratios should be characteristic of North Pacific Ocean waters (Eigl et al., 2017; Hain et al., 2020), low ratios (i.e., below 1×10^{-2} according to the Greenland Sea results reported in (Qiao, Hain, & Steier, 2020)) should be characteristic of AW since they have been in contact with RPs sources. The obtained results using the ^{233}U/^{236}U signature could complement the most recently reported information based on Ga concentration results (Whitmore et al., 2020) and the most conventional approach based on nitrate and phosphate concentration relationships (Peter Jones et al., 1998).

In a different context, another application would be the study of the U fingerprint in Deep and Bottom Waters (DBW) in the AO in which the anthropogenic influence can be considered negligible (E. P. Jones et al., 1995). ^{233}U and ^{236}U are naturally produced on the surface of rocks mainly from cosmic radiation induced neutrons (i.e., thermal neutron activation of ^{232}Th and ^{235}U, respectively). During surface wheathering some U is dissolved by oxygenated waters and the isotopic signal is eventually transported into the oceans (Dunk et al., 2002). Thanks to the long residence time of U in oceanic waters (i.e., 0.32–0.56 My (Dunk et al., 2002)), this isotopic signal should be preserved in the oldest water masses that can be found, for example, in the AO. The natural ^{233}U and ^{236}U inprint in these waters is expected to be characterized by extremely low ^{233}U and ^{236}U concentrations and ^{233}U/^{236}U ratios above that of anthropogenic sources (i.e., above 150×10^{-2}, see SI for further details). On the other hand, anthropogenic radionuclides might be present in DBW from either top-down diffusion and particle bound transport as observed for other GF radionuclides in the AO, thus altering the natural U signal (Macdonald & Carmack, 1990). The study of the ^{233}U and ^{236}U signatures in DBW in the AO could shed light on such processes and provide new insights into the U isotopic signature in natural waters in the AO.

In this work, we examine the potential of the ^{233}U/^{236}U atom ratio as a tool to disentangle water masses fingerprinted with different U sources in the AO. The study site is the western AO, sampled in 2015 during the GN01 US GEOTRACES expedition (Figure 1). Seawater samples collected at full-depth profiles in the Amerasian Basin allowed us to cover the widest possible range of ^{233}U and ^{236}U concentrations in the AO and to explore the ^{233}U/^{236}U signature for both natural and artificial U sources.
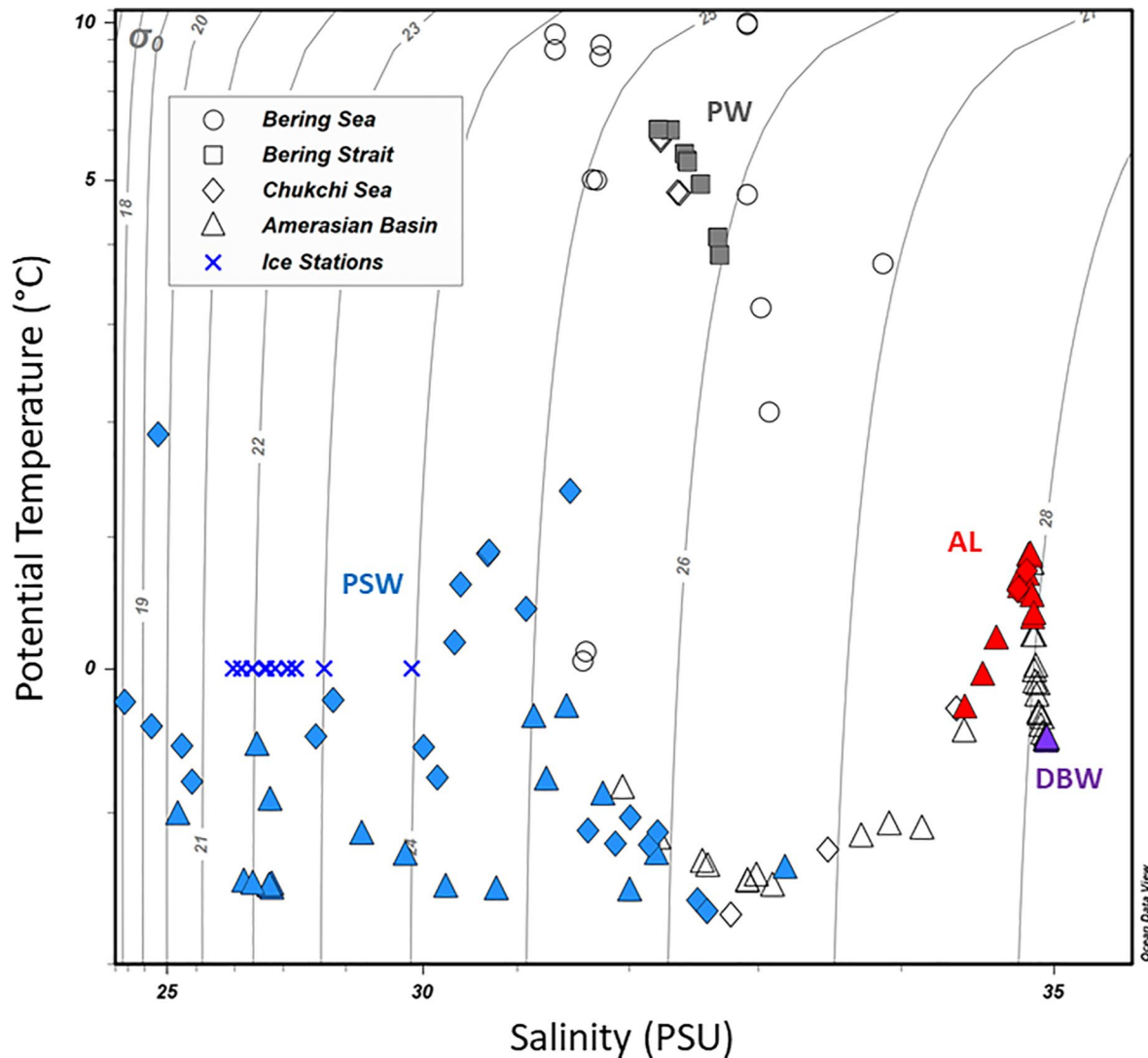
Figure 2. Temperature and Salinity properties of the studied samples grouped by geographical areas (Figure 1b) and color coded according to the distribution of water masses considered in this work: Pacific Waters, PW, in gray, corresponding to Bering Strait samples; Polar Surface Waters, PSW, in blue, representing the 0–100 depth interval; Atlantic Layer, AL, in red, corresponding to the 200–800 m depth range in the Chukchi Sea and Canada and Makarov Basins (Amerasian Basin); and Deep and Bottom Waters, DBW, in purple, for those samples below 2,000 m depth.

2. Materials and Methods

2.1. Sampling and Hydrographic Parameters

This study is based on samples taken during the GEOTRACES expedition onboard the US Coast Guard icebreaker *Healy*, which covered two main sections in the Amerasian Basin (GN01 section, Figure 1). In this work, 140 seawater samples from 22 stations were selected for the study of both ^{233}U and ^{236}U (Table S1 in Supporting Information S1). The selection of stations is based on profiles containing different water masses. Seawater sampling was carried out with 12 Niskin bottles of 30L each, and standard conductivity, temperature, and pressure sensors. Ice stations were sampled from small boat casts and Niskin bottles paired with McLane pumps. Samples were filtered by gravity through Teflon-lined *Tygon* tubing and *Supor Acropak 500* capsule filters (0.8/0.4 μm pore size), immediately acidified to pH 2 with distilled 6 M HCl and shipped to the Lamont Doherty Earth Observatory (LDEO) premises in New York (GEOTRACES cruise report, 2015).

The samples are further characterized according to their potential temperature and salinity (T-S plot, Figure 2). Bering Strait samples represent pure PW entering the AO, with salinities below 33 PSU and temperatures above

3°C. Polar Surface Waters (PSW) represent the layer where PW and AW, the latter circulating in the upper water column of the Eurasian Basin, might mix with melted sea-ice, river run-off and precipitation. Here all samples from the 0–100 m depth range were classified as PSW, exhibiting a wide range of salinities (i.e., between 22.8 and 33.2 PSU) and temperatures (i.e., −1.6°C–1.9°C). At the Amerasian Basin and the Chukchi Sea slope, the increase in salinity and potential temperature around 34.5 PSU and 0.5°C, respectively, indicates the presence of the core of AW circulating within the whole AO at middepth layers (i.e., Atlantic Layer, AL), assumed here to cover the 200–800 m depth and salinities above 34 PSU following the approximation given in (Wefing et al., 2021). Deep and Bottom Waters, DBW, with salinities close to 35 PSU and temperatures down to −0.5°C, are present at the deepest stations in the Amerasian Basin (i.e., below 2,000 m depth).

2.2. Radiochemistry and Measurements

The analysis of ^{236}U and ^{233}U concentrations was performed on 5L samples. Radiochemical sample preparation and AMS measurements were carried out as a collaborative effort between LDEO and the AMS facilities at ETH Zürich, Switzerland, and at the Centro Nacional de Aceleradores (CNA) in Seville, Spain. At the LDEO, U was concentrated by $Fe(OH)_3$ co-precipitation. The Fe precipitates were sent to CNA where the U was chemically purified based on the method from (López-Lora et al., 2018). Following the same working methodology adopted in (Villa-Alfageme et al., 2019), samples were divided in two groups for the analysis of the $^{233}U/^{238}U$ and $^{236}U/^{238}U$ atom ratios either at CNA on a 1 MV AMS system or at ETH on a 600 kV AMS facility. Details on the ^{236}U AMS measurement techniques at the ETH can be found in (Christl, Casacuberta, Lachner, et al., 2015) and at the CNA in (Chamizo & López-Lora, 2019). At both facilities U isotopes were measured using the oxide method, He gas was used as stripper, and U^{3+} ions were analyzed on the high-energy side with about 35% overall transmissions. The deepest samples from the Amerasian Basin, assumed to contain the lowest $^{236}U/^{238}U$ and $^{233}U/^{238}U$ atom ratios, were analyzed at ETH, where abundance sensitivities can reach the 10^{-13} level or below thanks to its optimized ion-beam design. The 1 MV CNA AMS system features a compact design which imposes restrictions to the minimum U atom ratios that can be measured (i.e., estimated at the 10^{-10} and 10^{-11} levels for $^{236}U/^{238}U$ and $^{233}U/^{238}U$ in seawater, respectively). Overall, 51 and 89 samples were prepared for their analysis at the CNA and ETH, respectively. Additionally, one procedural blank for every 10 processed samples (15 altogether) was prepared to control possible ^{233}U and ^{236}U contamination issues. New glassware and reagents of the highest purity were used during the sample processing to avoid background sources.

The AMS analysis of ^{233}U in 5L seawater samples is challenging because the expected $^{233}U/^{238}U$ atom ratios are at the 10^{-11} level and below, leading to very low ^{233}U count rates in all the samples. For example, even when assuming 100% chemical recovery and a quoted detection efficiency of 2×10^{-4} will lead to less than 100 registered ^{233}U counts from a 5L sample with a $^{233}U/^{238}U$ ratio of 10^{-11}, resulting in 1 sigma counting uncertainties of more than 10% for the measured $^{233}U/^{238}U$ ratio. Since instrumental instabilities are at the level of 1% and 2% at the ETH and CNA facilities, respectively, final uncertainties are dominated by counting statistics. To minimize and control the ^{233}U and ^{236}U AMS-related background problems, CNA and ETH AMS analyses were performed under clean ion-source conditions, and several instrumental blanks (i.e., unprocessed blank samples) were integrated in the measurement sequences. In-house standard materials were used to normalize the resulting $^{233}U/^{238}U$ and $^{236}U/^{238}U$ atom ratios (i.e., the ETH ZUTRI (Christl et al., 2013) and the CNA-U236 (Chamizo et al., 2015) standards). In general, procedural and instrumental blanks produced similar and reproducible ^{233}U and ^{236}U count rates. Background correction of the samples was performed by subtracting the number of ^{233}U (^{236}U) counts, given by the average number of counts of ^{233}U (^{236}U) of all blanks, from the total number of measured ^{233}U (^{236}U) counts (i.e., the integration time was the same for blanks and seawater samples). While the background correction for ^{236}U did not have a significant effect on most $^{236}U/^{238}U$ results, the net (background corrected) number of ^{233}U counts ranged between 1 and 40, which implies final relative 1 sigma counting uncertainties between 100% and 15% for the measured $^{233}U/^{238}U$ ratios, respectively. For 17 samples, only upper limits (on a 2 sigma level) for the $^{233}U/^{238}U$ ratios are provided because background corrected $^{233}U/^{238}U$ ratios were indistinguishable from zero.

Additionally, from each sample 5 ml seawater aliquots were collected by LDEO for ^{238}U analyses by Inductively Coupled Mass Spectrometry (ICP-MS) using the isotope dilution method at the CITIUS (Centro de Investigación Tecnológica e Innovación Universidad de Sevilla) premises, in Seville, Spain. The ^{238}U ICP-MS results were validated through the analysis a series of samples with well-known U isotopic compositions during the same
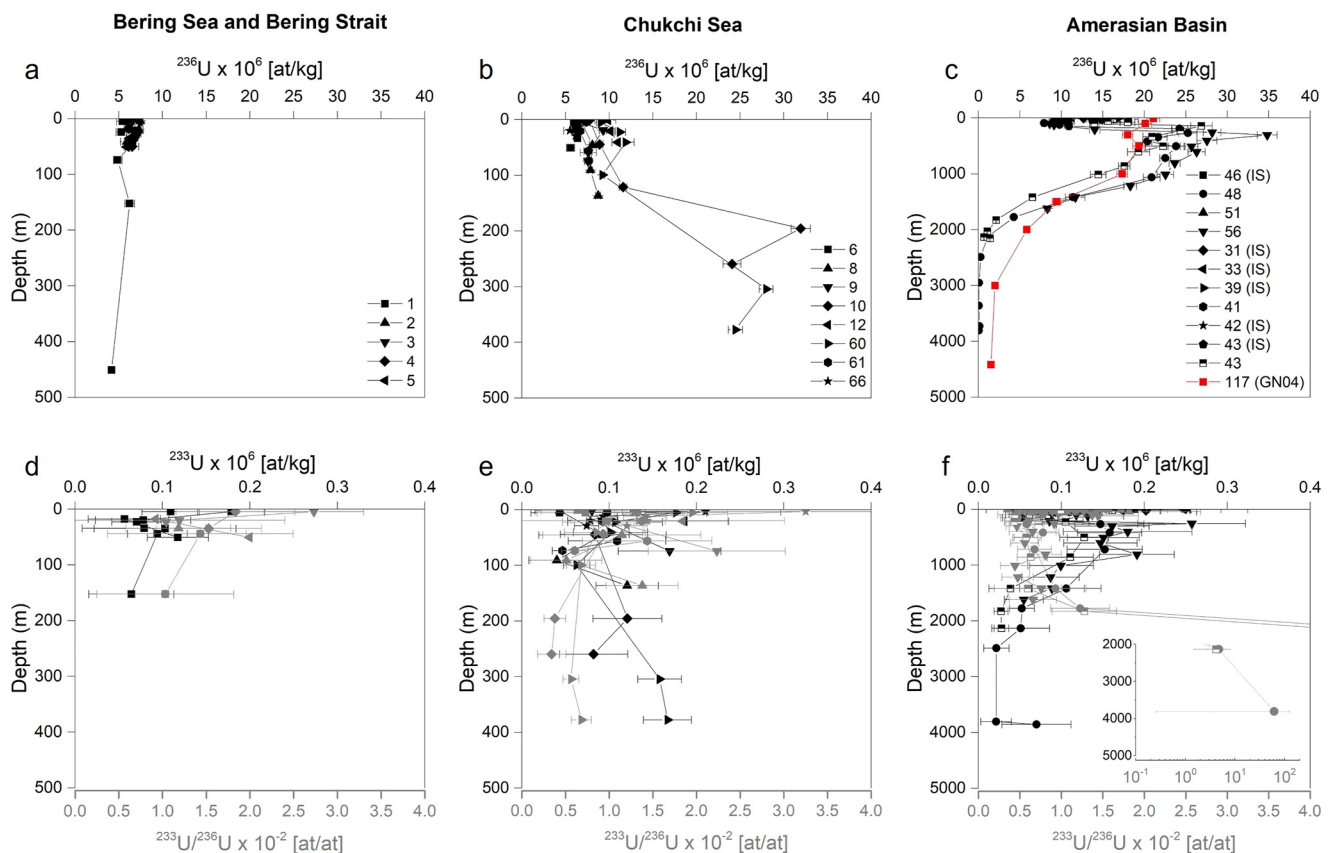
Figure 3. Obtained ^{236}U (a,b,c) and the ^{233}U (d,f,e) concentration depth profiles grouped by the geographical regions considered in this work (Figure 1b), including the results for the ice-stations (IS) in the Amerasian Basin. Plots d, e and g also include the obtained ^{233}U/^{236}U atom ratios (plotted in gray). Amerasian Basin ^{236}U plot (c) comprises also a depth profile from the Eurasian Basin for the purpose of data comparison (Stat. 117 from the GN04 GEOTRACES transect, red lines and symbols, from (Casacuberta et al., 2018)), and plot f includes an inset showing the ^{233}U/^{236}U ratios for the deepest samples. ^{236}U concentration results for Stat. 56 were reported in (Wefing et al., 2021). Part of the ^{236}U results for Stats. 43 and 48 at the Amerasian were published in (Mercedes López-Lora et al., 2021). Numerical values for the ^{233}U and ^{236}U concentrations can be found in Table S1 in Supporting Information S1.

sample batch. A comparison between the obtained ICP-MS results and the values predicted by salinity data using the formula given in (Owens et al., 2011) is presented in Figure S1 in Supporting Information S1. Only three samples produced unexpectedly high ^{238}U ICP-MS concentrations, which could be attributed to a contamination problem during the handling of the ICP-MS aliquots. For those three samples the results predicted by the salinity data were used instead of the ICP-MS data. The ^{238}U concentrations were used to calculate the ^{233}U and ^{236}U concentrations in the seawater samples using the ^{236}U/^{238}U and ^{233}U/^{238}U ratios from the AMS measurements (Table S1 in Supporting Information S1).

3. Results

The results in this work are grouped in three geographical regions: (a) Bering Sea and Bering Strait, (b) Chukchi Sea, and (c) Amerasian Basin, which includes the Makarov and the Canada Basins (including ice stations; Figure 1). The ^{236}U and ^{233}U concentration profiles and the calculated ^{233}U/^{236}U atom ratios are presented in Figure 3. Overall, ^{236}U concentrations range from $(0.035 \pm 0.017) \times 10^6$ to $(34.8 \pm 1.2) \times 10^6$ at/kg, and ^{233}U from $(0.016 \pm 0.007) \times 10^6$ to $(0.257 \pm 0.065) \times 10^6$ at/kg. Lowest concentrations of ^{236}U and ^{233}U may indicate the relative increase of the natural (pre-anthropogenic) U signal, with estimated, but never measured, values below 10^4 at/kg for both radionuclides (Peppard et al., 1952; Steier et al., 2008). The highest values clearly reflect the presence of anthropogenic U, with ^{236}U and ^{233}U concentrations at levels of 10^7 and 10^5 at/kg, respectively (Qiao, Hain, & Steier, 2020; Qiao, Zhang, et al., 2020). ^{233}U/^{236}U atom ratios show a very large variation, moving from $(0.34 \pm 0.16) \times 10^{-2}$ to values above 10×10^{-2}. The lowest ratio is still a factor of 3 higher compared to the
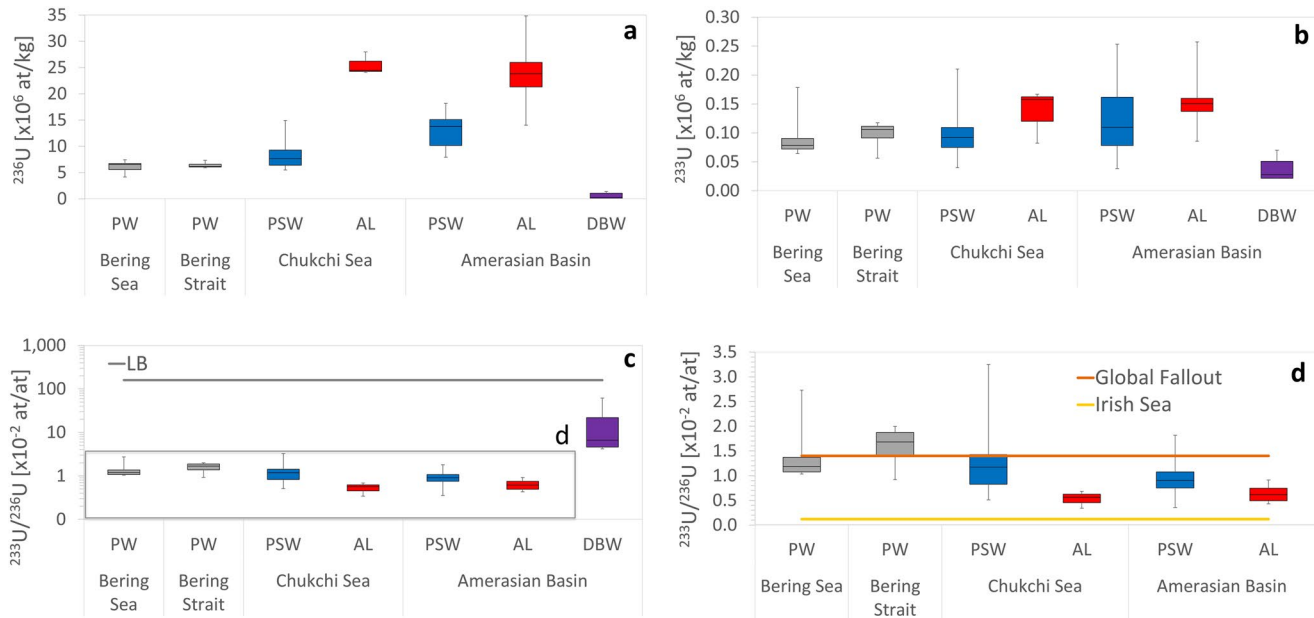
Figure 4. Boxplots showing the distribution of the obtained ^{233}U, ^{236}U and ^{233}U/^{236}U results for Bering Sea and Bering Strait samples (in gray), Polar Surface Waters (in blue), Atlantic Layer (in red) and Deep and Bottom Waters (in purple). Plot c includes the estimated ^{233}U/^{236}U atomic ratio in this work for pre-anthropogenic oceans or lithogenic background (LB), of about 150×10^{-2} (SI). Plot d includes the reported ^{233}U/^{236}U atomic ratios for global fallout, of $(1.40 \pm 0.15) \times 10^{-2}$, and as for the Irish Sea the weighted average for both seawater and sediment samples, of $(0.12 \pm 0.01) \times 10^{-2}$, has been considered (Hain et al., 2020).

weighted average of both Irish Sea seawater and sediment impacted by Sellafield RP discharges reported in (Hain et al., 2020), of $(0.12 \pm 0.01) \times 10^{-2}$, and is 20% lower than the average value for Greenland Sea surface seawater in the 2012–2016 time period reported in (Qiao, Hain, & Steier, 2020), of $(0.42 \pm 0.08) \times 10^{-2}$. The highest measured ratios, of $(8 \pm 6) \times 10^{-2}$ and $(61 \pm 61) \times 10^{-2}$, with large uncertainties due to the extremely low ^{233}U and ^{236}U involved concentrations, exceed all so far reported values in seawater samples.

The distribution of ^{236}U in seawater profiles (Figure 3a–3c) shows a different trend compared to ^{233}U (Figure 3d–3f). In the Bering Sea and Bering Strait concentrations of ^{236}U are relatively low (below 10×10^6 at/kg) and constant throughout all depths. In the Chukchi Sea, ^{236}U concentrations increase below 100 m depth. Deep profiles taken in the Canada and Makarov Basins (Amerasian Basin) show a peak of ^{236}U between 100 and 1,000 m depth, and a decreasing trend for greater depths. Profiles of ^{233}U similarly show higher values between 100 and 1,000 m depth at Amerasian Basin stations despite their large uncertainties. ^{233}U/^{236}U atom ratios (Figure 3d–3f) also show a trend toward lowest values at such depth range, but more remarkable is the increasing trend seen in the deepest samples of the basin stations (Figure 3f).

To investigate this further, samples were clustered by water masses according to the definitions given in Section 2.1, and the results expressed using boxplots in Figure 4. Bering Strait samples, representing PW inflowing into the AO, are characterized by median ^{236}U and ^{233}U concentrations of 6×10^6 and 0.1×10^6 at/kg, respectively, meaning a median ^{233}U/^{236}U atom ratio of 1.7×10^{-2}. In the Chukchi Sea, PSW exhibit a slightly higher median ^{236}U concentration, of 7.6×10^6 at/kg, but a similar ^{233}U value of 0.1×10^6 at/kg, giving a lower ^{233}U/^{236}U atom ratio, of 1.2×10^{-2}. At the Amerasian Basin, PSW show increasing and more scattered ^{236}U concentrations, reaching a median value of 14×10^6 at/kg, but still similar ^{233}U levels, going down the median ^{233}U/^{236}U atom ratio to a value of 0.9×10^{-2} (Figure 4c and 4d). The AL shows similar ^{236}U and ^{233}U median values both in the Chukchi Sea Shelf and in the Amerasian Basin, of about 24×10^6 and 0.15×10^6 at/kg, respectively, with a median ^{233}U/^{236}U atom ratio of 0.6×10^{-2}. The highest ^{236}U concentration observed in the western AO ($(34.8 \pm 1.2) \times 10^6$ at/kg for the sample at 305 m depth at Stat. 56 in the Canada Basin (see also Wefing et al., 2021)) exceeds the maximum concentrations reported for the entire eastern AO in 2015 ($(24 \pm 1) \times 10^6$ at/kg (Casacuberta et al., 2018)).

DBW in the Amerasian Basin exhibit the lowest ^{236}U and ^{233}U concentrations, with median values of 0.25×10^6 and 0.03×10^6 at/kg, respectively. The minimum measured ^{236}U concentration, $(0.03 \pm 0.02) \times 10^6$ at/kg, is 30
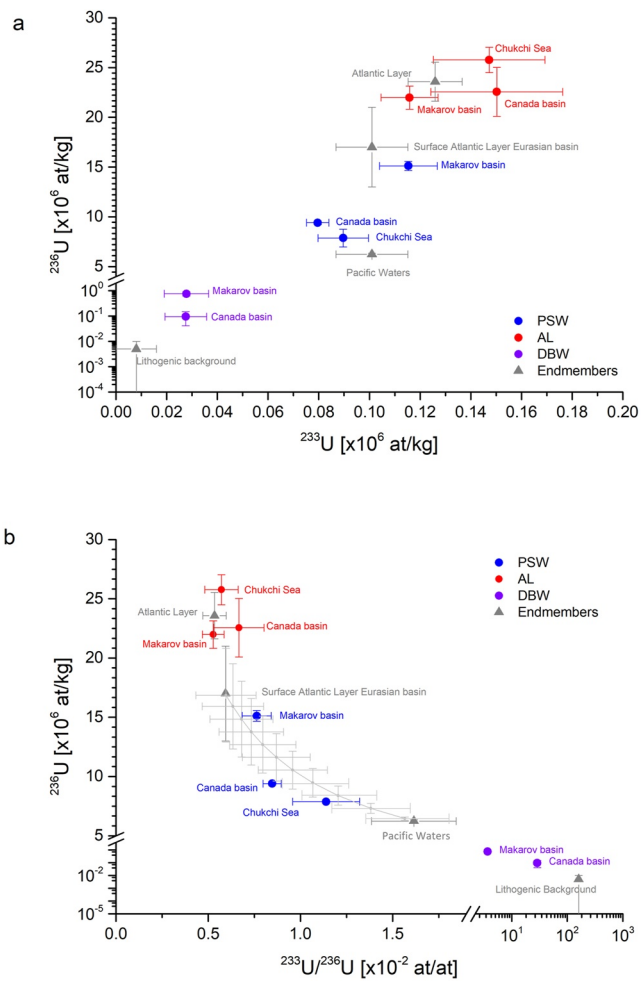
Figure 5. Average ^{236}U concentration versus average ^{233}U concentration (a), and average ^{236}U concentration versus average ^{233}U/^{236}U atomic ratio (b) by water mass and geographical area according to the description in Figure 1b. Endmember values for the most representative water masses have been also included (gray symbols, Table 1). In every case, error bars represent the standard deviation of the mean. Plot b includes the binary mixing line between Pacific and Atlantic Waters in Polar Surface Waters. In this case, error bars result from the error propagation of the individual endmember values.

times below the lowest documented value for the Eurasian Basin in (Casacuberta et al., 2018), of $(0.9 \pm 0.1) \times 10^6$ at/kg. The ^{233}U/^{236}U atom ratios measured in DBW, with a median value of 7×10^{-2}, are higher compared to those of both PSW and the AL.

4. Discussion

The average ^{236}U concentrations are plotted versus the average ^{233}U concentrations (Figure 5a) and versus mean ^{233}U/^{236}U atom ratios (Figure 5b) for every studied water mass and geographical area according to the description in Figure 1b. Based on our results three main conclusions are drawn and discussed in the following: (a) In PSW, PW can be unraveled from AW using the ^{233}U/^{236}U atomic ratio: (b) the AL has a distinct isotopic signal from PSW; and (c) the unexpectedly high ^{233}U/^{236}U atomic ratios in DBW reflect the relative increase of natural (pre-anthropogenic) U in the deep AO.

4.1. Polar Surface Waters

In the surface layer of the Amerasian Basin, PW flowing through the Bering Strait meet AW traveling through the eastern basin and reaching the western basin. Information on their mixing can be obtained if the results in this work are interpreted using the corresponding endmember values for those two water masses. Pure PW in this work is represented by Bering Strait samples, with average ^{236}U and ^{233}U concentrations of $(6.25 \pm 0.10) \times 10^6$ and $(0.10 \pm 0.02) \times 10^6$ at/kg, respectively, and an average ^{233}U/^{236}U atom ratio of $(1.62 \pm 0.25) \times 10^{-2}$ (Table 1). Surface Atlantic waters in the Eurasian Basin are mostly formed of AW entering the AO through the Fram Strait and the Barents Sea (Figure 1a). Using the ^{236}U concentration reported in (Casacuberta et al., 2018) for the surface layer (i.e., 10–35 m depth range) of the Eurasian Basin for also the 2015 sampling expedition, an average concentration of $(17 \pm 4) \times 10^6$ at/kg is assigned to this water mass. Note that the ^{236}U concentration in inflowing surface Atlantic Waters to the AO is time dependent (Christl, Casacuberta, Vockenhuber, et al., 2015), but in this work the above mentioned value was considered as a first approach to the problem. Due to a lack of experimental ^{233}U data for the Eurasian Basin, we assume that ^{233}U concentrations are like the values we measured in the Amerasian Basin, with a weighted average of $(0.10 \pm 0.02) \times 10^6$ at/kg. This assumption is supported by the fact that the measured ^{233}U concentrations in PSW in this work are in reasonable agreement with the reported concentrations for the West and East Greenland Sea in the period 2012–2016 in (Qiao,

Hain, & Steier, 2020), with an average value of $(0.07 \pm 0.01) \times 10^6$ at/kg, representing outflowing surface waters from the AO. Thus, the characteristic ^{233}U/^{236}U for the surface Atlantic layer in the Eurasian Basin is assumed to be $(0.60 \pm 0.15) \times 10^{-2}$ (Table 1). Note that the Eurasian Basin surface waters values are just estimations we consider in this work to explore the potential of ^{233}U/^{236}U as a water mass tracer in the AO. Future measurements of ^{233}U in seawater samples from the Eurasian Basin will help to better constrain this endmember for mixing calculations.

When looking at the concentrations of ^{233}U and ^{236}U (Figure 5a), results show that samples at the Chukchi Sea plot closer to the PW endmember values, whereas Makarov Basin values approach the endmember concentrations for the surface Atlantic Layer in the Eurasian Basin. ^{236}U average concentrations at the Canada Basin are roughly 30% higher compared to the Chukchi Sea, pointing to the presence of AW in the Canada Basin surface waters. The ^{233}U/^{236}U ratio decreases consistently from the Chukchi Sea to the Makarov Basin (Figure 5b). Canada Basin results plot in between the Makarov Basin and the Chukchi Sea. Drawing the mixing line between a hypothetical water mass of Pacific origin and another one representing pure surface AW in the Eurasian Basin, it is observed an increasing presence of AW in PSW from the Chukchi Sea to the Makarov Basin (Figure 5b). This estimation

Table 1
Estimated Endmembers Values for the ^{236}U and ^{233}U Concentrations and $^{233}U/^{236}U$ Atomic Ratio for the Water Masses in the Amerasian Basin

Water mass		^{236}U [$\times 10^6$ at/kg]		^{233}U [$\times 10^6$ at/kg]		$^{233}U/^{236}U$ [$\times 10^{-2}$ at/at]	
		Mean	Uncert.	Mean	Uncert.	Mean	Uncert.
Pacific Waters	Bering Strait results in this work	6.25	0.10	0.10	0.02	1.62	0.25
Surface Atlantic Layer in the Eurasian Basin	^{236}U result from the surface layer (0–35 m deep) in the Eurasian Basin in (Casacuberta et al., 2018). ^{233}U results from Polar Surface Waters in the Amerasian Basin in this work	17	4			0.60	0.15
Middepth Atlantic Layer in the Amerasian Basin	Results from this work	24	2	0.13	0.01	0.53	0.06
Deep and Bottom Waters (pre-anthropogenic oceans)	^{236}U data from (Steier et al., 2008). $^{233}U/^{236}U$ atom ratio estimated in this work assuming cosmogenic production in the surface of rocks (Lithogenic Background) (section SI)	5×10^{-3}	5×10^{-3}	8×10^{-3}	8×10^{-3}	150 (lower limit)	

Note. Uncertainties are expressed as standard deviations.

excludes the essentially tracer free waters (meteoric waters and sea ice melt), which could go up to 10%–20% (Paffrath et al., 2021). These results contrast with those worked out in (Whitmore et al., 2020): using the Ga concentration alone in samples corresponding also to the GN01 transect, almost negligible fractions of AW were identified at the Chukchi Sea and at the Canada Basin. The conclusions of our study represent a first best estimate using the $^{233}U/^{236}U$ atomic ratio as a fingerprint of water masses. Uncertainties underlying the characterization of the involved endmember values in both approaches might explain the different results. It is important to underline the solidity of the $^{233}U/^{236}U$ atomic ratio as a water mass tracer thanks to the long residence time of U in seawater (i.e., about 0.4 My (Dunk et al., 2002), two orders of magnitude longer than the one of Ga (Whitmore et al., 2020)) and the fact that isotopic ratios are not influenced by biogeochemical processes.

4.2. Atlantic Layer

Samples from the mid-depth AL in the Chukchi Sea, Canada Basin and Makarov Basin show about 3.5, 2.5 and 1.5 times, respectively, enhanced average ^{236}U concentrations compared to PSW. Overall AL ^{233}U values are about 30% above the measured ones in PSW (Figure 5a). The $^{233}U/^{236}U$ isotopic signals in the AL are thus distinct (Figure 5b). It can be observed that the obtained average results for the three investigated regions agree within uncertainties (Figures 5a and 5b). This means that the data obtained in this work can be used to establish representative values for the Atlantic Layer in the Amerasian Basin. Endmember values for the ^{236}U and ^{233}U concentrations are fixed to $(24 \pm 2) \times 10^6$ and $(0.13 \pm 0.01) \times 10^6$ at/kg, respectively, resulting in a $^{233}U/^{236}U$ atom ratio of $(0.53 \pm 0.06) \times 10^{-2}$ (Table 1). This atomic ratio would mean that roughly 60% of the ^{236}U in the AL in the western AO might come from RPs. The 30% enhanced ^{233}U signal in the AL compared to PSW could be explained considering the circulation time scales of AW in the AO. According to the simulations in (Christl, Casacuberta, Vockenhuber, et al., 2015), the GF ^{236}U and ^{233}U signals in the AW entering the AO would have peaked in the 1960s with a subsequent decaying trend reaching a steady level in the 1990s. Longer circulation times of AW in the AL compared to surface waters (i.e., of about 10 years, according to the results in (Wefing et al., 2021)) could explain the different ^{233}U signal. The higher ^{236}U levels in the AL compared to PSW might indicate either a more advective flow of AW reaching this basin compared to PSW, or releases of higher ^{236}U from Sellafield and La Hague RPs (Wefing et al., 2021). It is interesting to mention that the measured $^{233}U/^{236}U$ atomic ratios for the AL in this work, agree with the ones that can be modeled assuming the mixing of water streams upon entering the AO worked out in (Casacuberta et al., 2018; see Section 1 and Figure S2 in Supporting Information S1 for further details).

4.3. Deep and Bottom Waters

The extremely low ^{233}U and ^{236}U concentrations in DBW in the western basin (Figure 5-a) corroborates the long residence times of these waters and their isolation from the above layers (i.e., absence of convection of dense waters produced on the shelves; Macdonald & Carmack, 1990). More remarkable is, however, the behavior of

the ^{233}U/^{236}U atomic ratio, with average values pointing out to enhanced levels compared to waters masses above (Figure 5b). These numbers can be interpreted considering the presence of naturally occurring ^{233}U and ^{236}U.

Both ^{233}U and ^{236}U can be produced in situ in the lithosphere when thermalized neutrons, either from cosmic radiation or from radiogenic production, interact with the naturally present ^{232}Th (100% isotopic abundance) or ^{235}U (0.72% isotopic abundance), respectively. The U isotopic signal of eroding and chemically weathering lithogenic particles is transported into the sea either by direct deposition or through river runoff, with their average U isotopic fingerprint being finally detectable in pre-anthropogenic seawater (Dunk et al., 2002). Our theoretical estimations situate the ^{233}U/^{236}U atomic ratio at the level of $(25 \pm 2) \times 10^{-2}$ for the radiogenic production, whereas for the cosmogenic production a lower limit of 150×10^{-2} was estimated (see SI for further details). Both natural ratios are clearly distinguishable from GF, $(1.40 \pm 0.15) \times 10^{-2}$ (Hain et al., 2020). Since the cosmogenic production of both ^{233}U and ^{236}U dominates at the surface of eroding continents, we chose a ratio of 150×10^{-2} as representative for the lithogenic background. The measured values in the deep Canada and Makarov Basins, $(29 \pm 20) \times 10^{-2}$ and $(3.7 \pm 1.4) \times 10^{-2}$, respectively, are clearly shifted toward the estimated lithogenic background. The fact that none of the samples reached the estimated lithogenic background can be explained considering vertical mixing or particle transport carrying the anthropogenic U signal into the deepest waters since, as stated before, convection of dense waters produced on the shelves is not expected at these depths (Macdonald & Carmack, 1990). Although only three samples produced ^{233}U results above the limit of detection due to the extremely low levels involved, our results indicate a previously undiscovered trend in the ^{233}U/^{236}U atom ratio that could be used to distinguish pre-anthropogenic U in the oceans. More experimental data will shed light on this possible application.

5. Conclusions

This study explored the potential anthropogenic and natural ^{233}U and ^{236}U offer as a tracer of water sources and mixing of water bodies in the Arctic Ocean. Several water profiles were analyzed from a transect in the western Arctic Ocean. Concentrations of ^{233}U and ^{236}U were used to understand the main sources of anthropogenic uranium isotopes, and ^{233}U/^{236}U ratios helped comprehending the mixing of Pacific and Atlantic Waters in the Polar Surface Waters of the Amerasian Basin. ^{233}U, mostly originating from global fallout, shows relatively constant concentrations in modern waters, indicating a steady regional pattern. ^{236}U concentrations show distinct features in the water masses with an Atlantic influence reflecting the releases from European nuclear reprocessing plants. Thus, the main driver allowing the distinction of U sources using the ^{233}U/^{236}U ratio in the Arctic Ocean is ^{236}U concentration. Still, the ^{233}U/^{236}U ratios of samples clustered according to water mass and oceanic basins showing characteristic features that allow distinction between Polar Surface Waters, Atlantic Layer and Deep and Bottom Waters. The distribution of ^{233}U/^{236}U ratios in Polar Surface Waters reflects the mixing of Pacific and Atlantic waters, pointing out to a predominance of Pacific Waters at the Chukchi Sea and a non-negligible presence of Atlantic waters at the Canada Basin. However, a quantitative study of the water masses fractions was not possible due to underlying uncertainties in the source terms. The ^{233}U and ^{236}U fingerprints in the Atlantic layer are distinct from the ones in surface waters, and the average ^{233}U/^{236}U atom ratio, $(0.53 \pm 0.06) \times 10^{-2}$, indicates that roughly 60% of the anthropogenic inventory of ^{236}U comes from European nuclear reprocessing plants in that layer. Looking at the ^{233}U/^{236}U ratio in Deep and Bottom Waters we found an increase that is consistent with a gradual mixing with the natural lithogenic signal. If confirmed in future studies, the ^{233}U/^{236}U ratio in seawater can not only be used to distinguish the origin of an anthropogenic U contamination, but also allow the identification and the mixing with natural U sources. Future advances of both, analytical capabilities and knowledge of source terms, might improve the application of ^{233}U/^{236}U for the identification of water masses. The obvious advantage of this ratio is represented by the fact that two isotopes of the same element behave geochemically identically (and conservatively) in seawater. Thus, ^{233}U/^{236}U has the potential to become a robust water mass tracer that is less sensitive to many mixing processes.

Data Availability Statement

ICP-MS ^{238}U and AMS ^{236}U and ^{233}U concentration results for the studied samples in this work are accessible through the following link (Table S1 in Supporting Information S1).

References

Alkire, M. B., Morison, J., & Andersen, R. (2015). Variability in the meteoric water, sea-ice melt, and Pacific water contributions to the central Arctic Ocean, 2000-2014. *Journal of Geophysical Research: Oceans*, *120*(3), 1573–1598. https://doi.org/10.1002/2014JC010023

Alkire, M. B., Rember, R., & Polyakov, I. (2019). Discrepancy in the identification of the Atlantic/Pacific front in the central Arctic Ocean: NO versus nutrient relationships. *Geophysical Research Letters*, *46*(7), 3843–3852. https://doi.org/10.1029/2018GL081837

Årthun, M., Eldevik, T., & Smedsrud, L. H. (2019). The role of Atlantic heat transport in future Arctic winter sea ice loss. *Journal of Climate*, *32*(11), 3327–3341. https://doi.org/10.1175/JCLI-D-18-0750.1

Bullister, J. L. (2014). Atmospheric CFC-11, CFC-12, CFC-113, CCl4 and SF6 histories. Carbon Dioxide Information Analysis Center. https://doi.org/10.3334/CDIAC/otg.CFC_ATM_Hist_2014

Casacuberta, N., Christl, M., Vockenhuber, C., Wefing, A.-M., Wacker, L., Masqué, P., et al. (2018). Tracing the three Atlantic branches entering the Arctic Ocean with ^{129}I and ^{236}U. *Journal of Geophysical Research: Oceans*, *123*(9), 6909–6921. https://doi.org/10.1029/2018JC014168

Casacuberta, N., Masqué, P., Henderson, G., Rutgers van-der-Loeff, M., Bauch, D., Vockenhuber, C., et al. (2016). First ^{236}U data from the Arctic Ocean and use of ^{236}U/^{238}U and ^{129}I/^{236}U as a new dual tracer. *Earth and Planetary Science Letters*, *440*, 127–134. https://doi.org/10.1016/j.epsl.2016.02.020

Castrillejo, M., Witbaard, R., Casacuberta, N., Richardson, C. A., Dekker, R., Synal, H. A., & Christl, M. (2020). Unravelling 5 decades of anthropogenic 236U discharge from nuclear reprocessing plants. *The Science of the Total Environment*, *717*, 137094. https://doi.org/10.1016/j.scitotenv.2020.137094

Chamizo, E., & López-Lora, M. (2019). Accelerator mass spectrometry of ^{236}U with He stripping at the Centro Nacional de Aceleradores. *Nuclear Instruments and Methods in Physics Research Section B: Beam Interactions with Materials and Atoms*, *438*, 198–206. https://doi.org/10.1016/j.nimb.2018.04.020

Chamizo, E., Santos, F. J., López-Gutiérrez, J. M., Padilla, S., García-León, M., Heinemeier, J., et al. (2015). Status report of the 1 MV AMS facility at the Centro nacional de Aceleradores. *Nuclear Instruments and Methods in Physics Research Section B: Beam Interactions with Materials and Atoms*, *361*, 13–19. https://doi.org/10.1016/j.nimb.2015.02.022

Christl, M., Casacuberta, N., Lachner, J., Maxeiner, S., Vockenhuber, C., Synal, H.-A., et al. (2015). Status of ^{236}U analyses at ETH Zurich and the distribution of ^{236}U and ^{129}I in the North Sea in 2009. *Nuclear Instruments and Methods in Physics Research Section B: Beam Interactions with Materials and Atoms*, *361*(0), 510–516. https://doi.org/10.1016/j.nimb.2015.01.005

Christl, M., Casacuberta, N., Vockenhuber, C., Elsaasser, C., Pascal Bailly, d.B., Herrmann, J., & Synal, H.-A. (2015). Reconstruction of the ^{236}U input function for the Northeast Atlantic Ocean: Implications for ^{129}I/^{236}U and ^{236}U/^{238}U-based tracer ages. *Journal of Geophysical Research: Oceans*, *120*(11), 7282–7299. https://doi.org/10.1002/2015JC011116

Christl, M., Vockenhuber, C., Kubik, P. W., Wacker, L., Lachner, J., Alfimov, V., & Synal, H. A. (2013). The ETH Zurich AMS facilities: Performance parameters and reference materials. *Nuclear Instruments and Methods in Physics Research Section B: Beam Interactions with Materials and Atoms*, *294*, 29–38. https://doi.org/10.1016/J.NIMB.2012.03.004

Doney, S. C., Jenkins, W. J., & Bullister, J. L. (1997). A comparison of tracer dating techniques on a meridional section in the eastern North Atlantic. *Deep-Sea Research I*, *44*(4), 603–626. https://doi.org/10.1016/s0967-0637(96)00105-7

Dorsey, H. G., & Peterson, W. H. (1976). Tritium in the Arctic Ocean and East Greenland current. *Earth and Planetary Science Letters*, *32*(2), 342–350. https://doi.org/10.1016/0012-821X(76)90074-1

Dunk, R. M., Mills, R. A., & Jenkins, W. J. (2002). A reevaluation of the oceanic uranium budget for the Holocene. *Chemical Geology*, *190*(1–4), 45–67. https://doi.org/10.1016/S0009-2541(02)00110-9

Eigl, R., Steier, P., Sakata, K., & Sakaguchi, A. (2017). Vertical distribution of ^{236}U in the North Pacific Ocean. *Journal of Environmental Radioactivity*, *169–170*, 70–78. https://doi.org/10.1016/J.JENVRAD.2016.12.010

GEOTRACES cruise report. (2015). GN01 SECTION – CRUISE HLY1502, ARCTIC OCEAN. Retrieved from https://www.geotraces.org/gn01/

Hain, K., Steier, P., Froehlich, M. B., Golser, R., Hou, X., Lachner, J., et al. (2020). ^{233}U/^{236}U signature allows to distinguish environmental emissions of civil nuclear industry from weapons fallout. *Nature Communications*, *11*(1), 1–3. https://doi.org/10.1038/s41467-020-15008-2

Hardy, E. P., Krey, P. W., & Volchock, H. L. (1973). Global inventory and distribution of fallout plutonium. *Nature*, *241*(5390), 444–445. https://doi.org/10.1038/241444a0

HELCOM MORS Discharge database. (n.d.). Helsinki Commission (HELCOM) [dataset]. Retrieved from https://helcom.fi/baltic-sea-trends/data-maps/databases/

Ho, M., Obbard, E., Burr, P. A., & Yeoh, G. (2019). A review on the development of nuclear power reactors. *Energy Procedia*, *160*, 459–466. https://doi.org/10.1016/j.egypro.2019.02.193

Holliday, N. P., Bersch, M., Berx, B., Chafik, L., Cunningham, S., Florindo-López, C., et al. (2020). Ocean circulation causes the largest freshening event for 120 years in eastern subpolar North Atlantic. *Nature Communications*, *11*(1), 1–15. https://doi.org/10.1038/s41467-020-14474-y

Jones, E. P., Anderson, L. G., & Swift, J. H. (1998). Distribution of Atlantic and Pacific waters in the upper Arctic Ocean: Implications for circulation. *Geophysical Research Letters*, *25*(6), 765–768. https://doi.org/10.1029/98GL00464

Jones, E. P., Rudels, B., & Anderson, L. G. (1995). Deep waters of the Arctic Ocean: Origins and circulation. *Deep-Sea Research Part I*, *42*(5), 737–760. https://doi.org/10.1016/0967-0637(95)00013-V

López-Lora, M., Chamizo, E., Levy, I., Christl, M., Casacuberta, N., & Kenna, T. C. (2021). ^{236}U, ^{237}Np and ^{239,240}Pu as complementary fingerprints of radioactive effluents in the Western Mediterranean Sea and in the Canada Basin (Arctic Ocean). *The Science of the Total Environment*, *765*, 142741. https://doi.org/10.1016/J.SCITOTENV.2020.142741

López-Lora, M., Chamizo, E., Villa-Alfageme, M., Hurtado-Bermúdez, S., Casacuberta, N., & García-León, M. (2018). Isolation of ^{236}U and ^{239,240}Pu from seawater samples and its determination by accelerator mass spectrometry. *Talanta*, *178*, 202–210. https://doi.org/10.1016/j.talanta.2017.09.026

Macdonald, R. W., Carmack, E. C., & Wallace, D. W. R. (1990). Tritium and radiocarbon dating of Canada Basin deep waters. *Science*, *259*(January), 1–2. https://doi.org/10.1126/science.259.5091.103

Naegeli, R. E. (2004). *Calculation of the radionuclides in PWR spent fuel samples for SFR experiment planning* (SANDIA Report, SAND2004-2757). Retrieved from http://prod.sandia.gov/techlib/access-control.cgi/2004/042757.pdf

Owens, S. A., Buesseler, K. O., & Sims, K. W. W. (2011). Re-evaluating the 238U-salinity relationship in seawater: Implications for the 238U–234Th disequilibrium method. *Marine Chemistry*, *127*(1–4), 31–39. https://doi.org/10.1016/j.marchem.2011.07.005

Paffrath, R., Laukert, G., Bauch, D., Rutgers Van Der Loeff, M., & Pahnke, K. (2021). Separating individual contributions of major Siberian rivers in the Transpolar Drift of the Arctic Ocean. *Scientific Reports*, *11*, 8216. https://doi.org/10.1038/s41598-021-86948-y

Peppard, D. F., Mason, G. W., Gray, P. R., & Mech, J. F. (1952). Occurrence of the (4n + 1) series in nature. *Journal of the American Chemical Society*, *74*(23), 6081–6084. https://doi.org/10.1021/ja01143a074

Qiao, J., Hain, K., & Steier, P. (2020). First dataset of ^{236}U and ^{233}U around the Greenland coast: A 5-year snapshot (2012–2016). *Chemosphere*, *257*. 127185. https://doi.org/10.1016/j.chemosphere.2020.127185

Qiao, J., Zhang, H., Steier, P., Hain, K., Henderson, G., Eriksson, M., et al. (2020). A previously unknown source of reactor radionuclides in the Baltic Sea, identified by ^{233,236,238}U and ^{127,129}I multi-fingerprinting. *Nature Communications*. *12*, 823. https://doi.org/10.1038/s41467-021-21059-w

Rahmstorf, S., Box, J. E., Feulner, G., Mann, M. E., Robinson, A., Rutherford, S., & Schaffernicht, E. J. (2015). Exceptional twentieth-century slowdown in Atlantic Ocean overturning circulation. *Nature Climate Change*, *5*(5), 475–480. https://doi.org/10.1038/nclimate2554

Sakaguchi, A., Kadokura, A., Steier, P., Takahashi, Y., Shizuma, K., Hoshi, M., et al. (2012). Uranium-236 as a new oceanic tracer: A first depth profile in the Japan Sea and comparison with caesium-137. *Earth and Planetary Science Letters*, *333–334*, 165–170. https://doi.org/10.1016/j.epsl.2012.04.004

Sakaguchi, A., Kawai, K., Steier, P., Quinto, F., Mino, K., Tomita, J., et al. (2009). First results on236U levels in global fallout. *The Science of the Total Environment*, *407*(14), 4238–4242. https://doi.org/10.1016/j.scitotenv.2009.01.058

Smith, J. N., McLaughlin, F. A., Smethie, W. M., Moran, S. B., & Lepore, K. (2011). Iodine-129, ^{137}Cs, and CFC-11 tracer transit time distributions in the Arctic Ocean. *Journal of Geophysical Research*, *116*(C4), C04024. https://doi.org/10.1029/2010JC006471

Steier, P., Bichler, M., Keith Fifield, L., Golser, R., Kutschera, W., Priller, A., et al. (2008). Natural and anthropogenic 236U in environmental samples. *Nuclear Instruments and Methods in Physics Research Section B: Beam Interactions with Materials and Atoms*, *266*(10), 2246–2250. https://doi.org/10.1016/j.nimb.2008.03.002

Tanhua, T., Jones, E. P., Jeansson, E., Jutterström, S., Smethie, W. M., Wallace, D. W. R., & Anderson, L. G. (2009). Ventilation of the arctic ocean: Mean ages and inventories of anthropogenic CO_2 and CFC-11. *Journal of Geophysical Research: Oceans*, *114*(1), C01002. https://doi.org/10.1029/2008JC004868

UNSCEAR. (2000). Exposures from man-made sources of radiation. Report. In *Sources and effect of ionizing radiation*. Annex C. (Vol. I). UNSCEAR.

Villa-Alfageme, M., Chamizo, E., Kenna, T. C., López-Lora, M., Casacuberta, N., Chang, C., et al. (2019). Distribution of ^{236}U in the U.S. GEOTRACES Eastern Pacific Zonal Transect and its use as a water mass tracer. *Chemical Geology*, *517*, 44–57. https://doi.org/10.1016/j.chemgeo.2019.04.003

Wefing, A. M., Casacuberta, N., Christl, M., Gruber, N., & Smith, J. N. (2021). Circulation timescales of Atlantic water in the Arctic Ocean determined from anthropogenic radionuclides. *Ocean Science*, *17*(1), 111–129. https://doi.org/10.5194/os-17-111-2021

Weiss, W., & Roether, W. (1980). The rates of tritium input to the world oceans. *Earth and Planetary Science Letters*, *49*(2), 435–446. https://doi.org/10.1016/0012-821X(80)90084-9

Whitmore, L. M., Pasqualini, A., Newton, R., & Shiller, A. M. (2020). Gallium: A new tracer of Pacific water in the Arctic Ocean. *Journal of Geophysical Research: Oceans*, *125*(7), 1–17. https://doi.org/10.1029/2019JC015842

Winkler, S. R., Steier, P., & Carilli, J. (2012). Bomb fall-out ^{236}U as a global oceanic tracer using an annually resolved coral core. *Earth and Planetary Science Letters*, *359*(360), 124–130. https://doi.org/10.1016/J.EPSL.2012.10.004

Woodgate, R. A., Weingartner, T., & Lindsay, R. (2010). The 2007 Bering Strait oceanic heat flux and anomalous Arctic sea-ice retreat. *Geophysical Research Letters*, *37*(1), 1–5. https://doi.org/10.1029/2009GL041621

References From the Supporting Information

Alfimov, V., & Ivy-Ochs, S. (2009). How well do we understand production of 36Cl in limestone and dolomite? *Quaternary Geochronology*, *4*(6), 462–474. https://doi.org/10.1016/j.quageo.2009.08.005

IAEA, MARIS. (2021).IAEA marine radioactivity information system. In *Division of IAEA environment laboratories*. [online]. Retrieved from. https://maris.iaea.org/explore/type/1/ref/685